



Obrabotka metallov -

Metal Working and Material Science



Journal homepage: [http://journals.nstu.ru/obrabotka\\_metallov](http://journals.nstu.ru/obrabotka_metallov)



## Martensitic transformations in TiNi-based alloys during rolling with pulsed current

Anna Misochenko<sup>a, \*</sup>

A.A. Blagonravov Mechanical Engineering Research Institute of the Russian Academy of Sciences, 4 Maly Kharitonievsky per., Moscow, 101990, Russian Federation

<sup>a</sup>  <https://orcid.org/0000-0002-2885-1996>,  [ls3216@yandex.ru](mailto:ls3216@yandex.ru)

### ARTICLE INFO

#### Article history:

Received: 11 December 2024

Revised: 09 January 2025

Accepted: 10 April 2025

Available online: 15 June 2025

#### Keywords:

TiNi-based alloys

Pulsed current

Current-assisted rolling

Martensitic transformations

X-ray diffraction analysis

Austenite stabilization

Cyclic martensitic transformation

### ABSTRACT

**Introduction.** Shape memory alloys based on TiNi possess a set of properties, including biocompatibility, corrosion resistance, low density, high specific strength, thermal stability, shape memory effect, and superelasticity. A significant number of studies are currently dedicated to various deformation methods of processing such materials, aiming to enhance their mechanical properties and shape memory characteristics. One such method is plastic deformation with the simultaneous application of pulsed current. Since the shape memory properties in TiNi-based alloys are due to the presence of thermoelastic martensitic transformations, the combined effect of deformation and current on these transformations is of particular interest. **The purpose** of this work is to investigate the characteristics of thermal and deformation-induced martensitic transformations in  $Ti_{50.0}Ni_{50.0}$  and  $Ti_{49.2}Ni_{50.8}$  alloys during rolling with simultaneous application of pulsed current. **Research methods.** The paper analyzes samples of  $Ti_{50.0}Ni_{50.0}$  and  $Ti_{49.2}Ni_{50.8}$  alloys after rolling with pulsed current at a density of 100 A/mm<sup>2</sup>, a pulse duration of 100 μs, a pulse ratio of 10 to various strain levels ( $\varepsilon = 0; 0.4; 0.8; 1.2$ ). The study of the staging of martensitic transformations was carried out using differential scanning calorimetry at a heating/cooling rate of 10 °C/min in the temperature range of –150 to +150 °C. The phase composition was studied by X-ray diffraction analysis using Cu-K $\alpha$  radiation at  $U = 40$  kV and  $I = 40$  mA in the angular range of  $2\theta = 15$  to 100 ° with a step size of  $\Delta\theta = 0.05^\circ$  and an exposure time of 5 s. **Results and discussion.** The results show that current-assisted rolling leads to the manifestation of a two-stage direct martensitic transformation during cooling in both alloys. Furthermore, increasing the strain level broadens the temperature range of the R-phase existence. The possibility of stabilizing the high-temperature austenitic B2 phase in the  $Ti_{49.2}Ni_{50.8}$  alloy, as well as the emergence of a cyclically occurring deformation-induced “martensite-austenite-martensite” transformation in the  $Ti_{50.0}Ni_{50.0}$  alloy, are demonstrated. Possible mechanisms for these features are discussed.

**For citation:** Misochenko A.A. Martensitic transformations in TiNi-based alloys during rolling with pulsed current. *Obrabotka metallov (tekhnologiya, oborudovanie, instrumenty)* = *Metal Working and Material Science*, 2025, vol. 27, no. 2, pp. 255–269. DOI: 10.17212/1994-6309-2025-27.2-255-269. (In Russian).

## Introduction

TiNi-based shape memory alloys possess a unique set of properties, including low density, biocompatibility, corrosion resistance, high specific strength, ductility, and strain reversibility under heating (shape memory) and upon unloading without heating (superelasticity) [1]. A large number of studies are currently devoted to various deformation methods in order to improve the mechanical and shape memory properties of such materials [2–4]. However, traditional metal forming processes without heating often lead to the destruction of these alloys. Therefore, the current standard technology for manufacturing semi-finished products from these alloys involves the use of warm and hot deformation [5, 6]. In turn, increasing the deformation temperature leads to a decrease in strength [6, 7]. Some works [8, 9] indicate that it is possible to avoid this problem when using pulsed electric current during plastic deformation, which leverages the electroplastic

#### \* Corresponding author

Misochenko Anna., Ph.D. (Engineering), Senior Researcher

A. A. Blagonravov Mechanical Engineering Research Institute of the Russian Academy of Sciences,

4 Maly Kharitonievsky per.,

101990, Moscow, Russian Federation

Tel.: +7 916 361-48-63, e-mail: [ls3216@yandex.ru](mailto:ls3216@yandex.ru)

effect (*EPE*). Studies on the application of *EPE* include rolling [10, 11], drawing [12], bending [13], microforming [12, 14], extrusion [15], and compression [16]. However, deformation behavior studies of various materials (pure metals and alloys) under tension are the most widely used [14, 17]. The specific deformation behavior of shape memory alloys, and their differences from traditional metals under tension with current, is detailed in [8, 18]. Studies on *TiNi* samples during rolling with current have shown an increase in deformability [19, 20] and mechanical properties [21]. In addition, it has been shown that it is possible to obtain a nanostructure (*NS*) [19] and increase the reversible strain and superelasticity [22] by using pulsed current-assisted rolling. The formation of *NS* is also possible in these alloys by using electric pulse treatment instead of traditional post-deformation annealing [23].

The specific effects of the electric current on the structure in various deformation schemes in different metals and alloys are described in [24, 25]. It is noted that the supply of electrical energy usually leads to structural changes, such as a decrease in dislocation density [26], the appearance of twins [27], dynamic recrystallization [28], grain refinement [29], the evolution of crystallographic texture [30], and the formation of oriented microstructures [31, 32], as well as particle redistribution and aging [33]. However, in shape memory alloys, the current can also affect the martensitic transformations (*MTs*). The possibility of controlling phase transformations by using current during rolling is shown in [34]. This paper compares the appearance of *MTs* in *TiNi* alloy after cold rolling and pulsed current-assisted rolling. At the same time, there is a lower intensity of deformation processes (relaxation mechanism) when using electrical current. For example, it has been shown that cold rolling can lead to *MT* suppression, while using current at the same strain leads to its manifestation.

Although the heating during rolling with current of *TiNi* alloys (at a density of no more than 100 A/mm<sup>2</sup>, a rate of 5 cm/sec, and a sample length of 10 cm) does not exceed 50-70 °C [35], it is localized and insignificant for the dynamic recrystallization processes. However, this temperature can have a significant effect on the *MTs*, which are the main characteristics of shape memory alloys.

The **purpose** of this work is to study the features of thermal and strain-induced martensitic transformations in *TiNi*-based alloys during rolling with electrical current. To achieve this purpose, the following **tasks** were solved during the research:

- analyzing thermal martensitic transformations in *Ti*<sub>50.0</sub>*Ni*<sub>50.0</sub> and *Ti*<sub>49.2</sub>*Ni*<sub>50.8</sub> alloys after pulsed current-assisted rolling to various strains using calorimetry;
- analyzing deformation-induced martensitic transformations in *Ti*<sub>50.0</sub>*Ni*<sub>50.0</sub> and *Ti*<sub>49.2</sub>*Ni*<sub>50.8</sub> alloys during pulsed current-assisted rolling using X-ray diffraction phase analysis;
- analyzing structural states in *Ti*<sub>50.0</sub>*Ni*<sub>50.0</sub> and *Ti*<sub>49.2</sub>*Ni*<sub>50.8</sub> alloys during pulsed current-assisted rolling.

## Research methods

The objects of the study were hot-rolled bars with a diameter of 6 mm and a length of 100 mm, made from *Ti*<sub>50.0</sub>*Ni*<sub>50.0</sub> and *Ti*<sub>49.2</sub>*Ni*<sub>50.8</sub> alloys. The average grain size in the initial state was 30 μm for *Ti*<sub>50.0</sub>*Ni*<sub>50.0</sub> and 60 μm for *Ti*<sub>49.2</sub>*Ni*<sub>50.8</sub>. After quenching from 800 °C in water, the alloys exhibited a predominant structure of *B19'* martensite and *B2* austenite, respectively, at room temperature (*T<sub>r</sub>*). The characteristic temperatures of the martensitic transformations are shown in Table.

The samples were subjected to rolling with electrical current at room temperature until they reached true strains of  $\epsilon = 0.4, 0.8, \text{ and } 1.4$  ( $\epsilon = \ln(S_0/S_f)$ , where  $\epsilon$  is the true strain, and  $S_0$  and  $S_f$  are the initial and final cross-sectional areas before and after rolling, respectively). Rolling was carried out on a rolling mill with calibrated rolls, using a single compression of 50 μm per pass and a rolling rate of 5 cm/s. The caliber sizes ranged from 1 to 7 mm. The rolling mill was equipped with a pulsed current generator. The current pulses were applied to the deformation zone using a sliding contact (negative pole) and to one of the rolls (positive pole), as shown in Fig. 1, with a frequency of 1,000 Hz and a duty cycle of 10. The amplitude current density was  $j = 100 \text{ A/mm}^2$ , and the pulse duration was  $100 \times 10^{-6} \text{ s}$ . Sample heating was monitored using an alumel-chromel thermocouple while passing current without deformation. The temperature increase was no more than 50-70 °C. The sample was under current for no more than 2 seconds. After each pass, the

## Characteristic temperatures of martensitic transformations

Alloy	Initial processing	Direct martensitic transformation $C2 \rightarrow B19'$		Reverse martensitic transformation $B19' \rightarrow C2$		Phase composition at room temperature
		$M_s$ , °C	$M_f$ , °C	$A_s$ , °C	$A_f$ , °C	
$Ti_{49.2}Ni_{50.8}$	Quenching (water) 800 °C (1 hour)	-5 °	-37	-5	17	austenite C2
$Ti_{50.0}Ni_{50.0}$		45	25	58	77	martensite C19'

$M_s$ , °C – the direct martensitic transformation ( $B2 \rightarrow B19'$ ) start temperature;

$M_f$ , °C – the direct martensitic transformation finish temperature;

$A_s$ , °C – the reverse martensitic transformation ( $B2 \rightarrow B19'$ ) start temperature;

$A_f$ , °C – the reverse martensitic transformation finish temperature.

samples were cooled in water to avoid additional current heating. Post-deformation annealing, when necessary, was carried out at 450 °C for 1 hour after rolling.

Thermal martensitic transformation temperatures were studied by differential scanning calorimetry (DSC) using a Mettler Toledo 822e apparatus. Calorimetric curves were obtained in the temperature range from -150 to 150 °C with a heating/cooling rate of 10 °C/min. Strain-induced martensitic transformations were studied by performing phase analysis on the samples after rolling with current to different strains. X-ray diffraction phase analysis was performed using an ARL X'TRA X-ray diffractometer (Switzerland) with Cu K $\alpha$  radiation in the angle range  $2\theta = 15-100^\circ$  with a step size of  $\Delta\theta = 0.05^\circ$  and an exposure time of 5 s at a voltage  $U = 40$  kV and a current  $I = 40$  mA. Qualitative phase assessment was carried out using the WinXRD computer software package (ARL X'tra software) by comparing it with the database of the International Centre for Diffraction Data (ICDD) PDF-2 [36]. Structural studies after rolling were carried out by transmission electron microscopy (TEM) using a high-resolution JEM 2100 microscope from JEOL (Japan) at a maximum accelerating voltage of 200 kV.

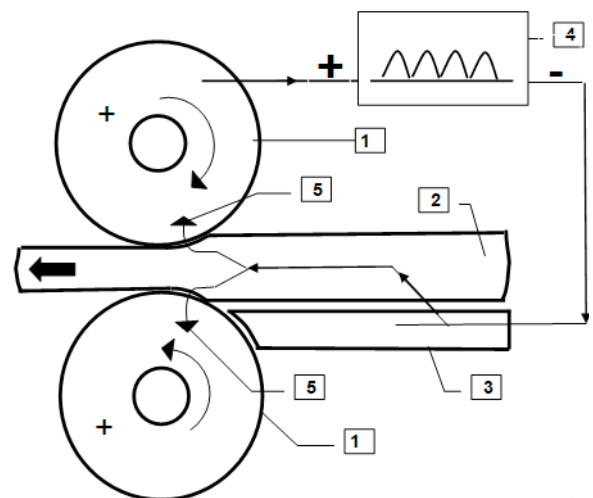


Fig. 1. Schematic of current supply circuit:  
1 – mill rolls; 2 – cylindrical sample; 3 – feed table (sliding contact); 4 – pulsed current source; 5 – current lines

## Results and discussion

The calorimetric studies of the  $Ti_{50.0}Ni_{50.0}$  alloy after pulsed current-assisted rolling and annealing at 450 °C showed the presence of a two-stage MT with an intermediate **R**-phase (Fig. 2, a). This phase is common in nickel-enriched alloys [37], but some authors observe it in  $Ti_{50.0}Ni_{50.0}$  alloys and attribute its presence to high internal stresses, for example, after thermal cycling [38] or plastic deformation [39]. In the  $Ti_{49.2}Ni_{50.8}$  alloy, the **R**-phase is observed immediately after annealing in the undeformed state, and it is associated with the presence of  $Ti_3Ni_4$  particles [37]. While there is no shift in the **B2**→**R** MT start temperatures, a shift in the **R**→**B19'** start temperature is noticeable (Fig. 2, b). This effect, where the pulsed current expands the **R**-phase temperature range, is also observed when comparing MTs with the initial undeformed state.

A characteristic feature of TiNi-based alloys is that MTs manifest not only during cooling and heating but also during deformation [37]. According to X-ray diffraction analysis, all peaks in the diffraction pattern of the  $Ti_{50.0}Ni_{50.0}$  alloy in the initial quenched state correspond to the **B19'** martensitic phase with a monoclinic lattice (Fig. 3, a). Cold rolling without current leads to a reverse martensitic transformation. Consequently,

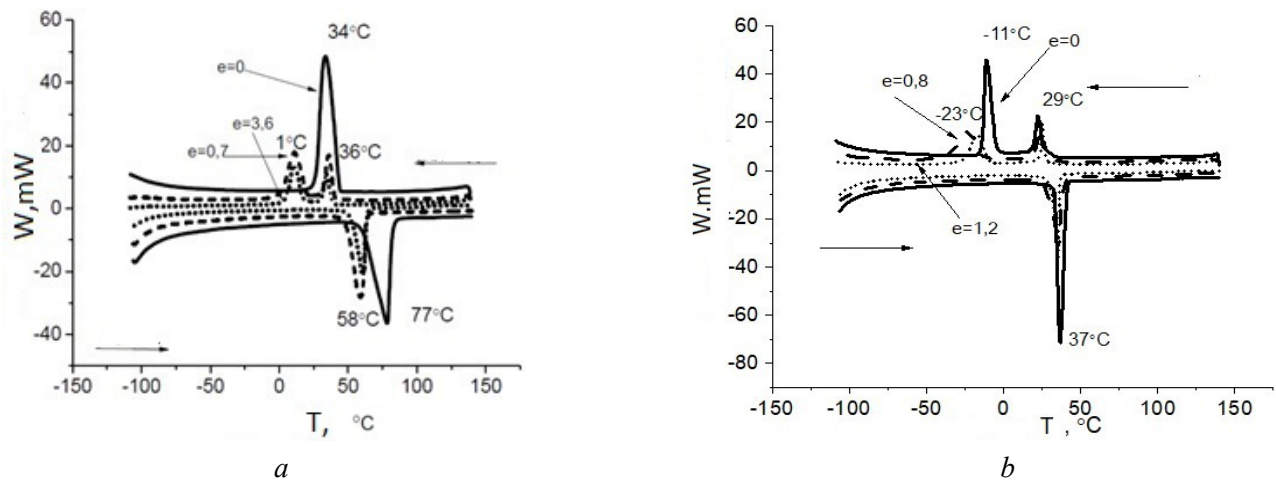
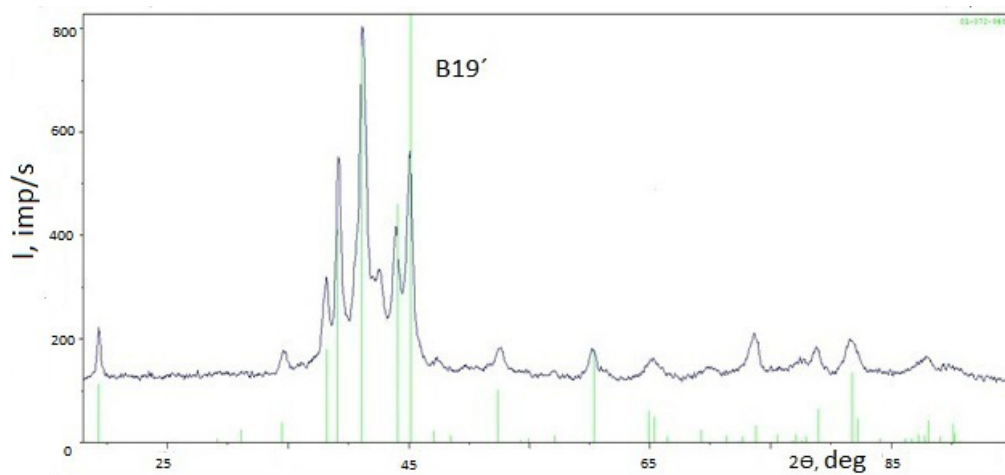
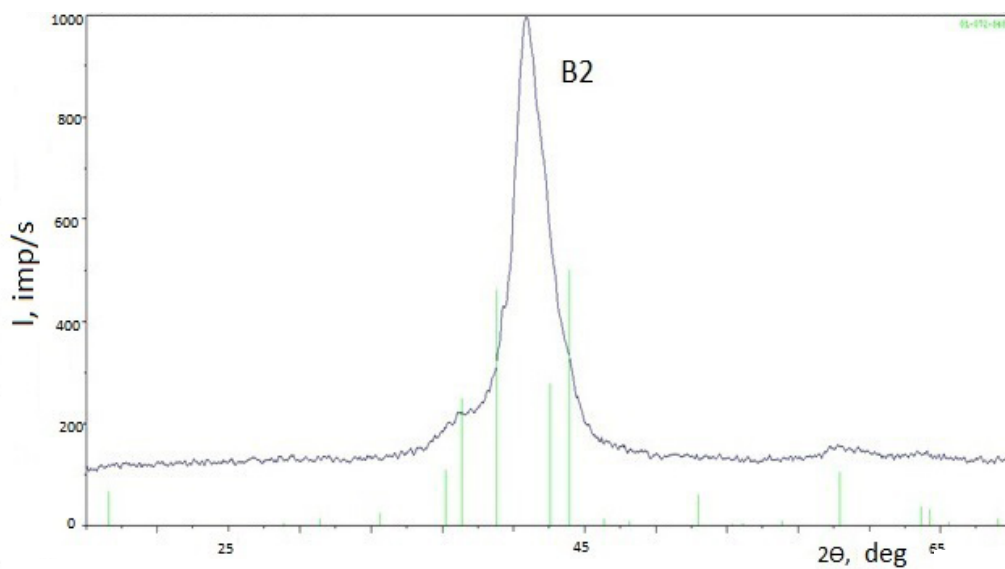


Fig. 2. Phase transitions in  $Ti_{50.0}Ni_{50.0}$  (a) and  $Ti_{49.2}Ni_{50.8}$  (b) alloys after current-assisted rolling in the annealed state (450 °C)



a



b

Fig. 3. X-ray diffraction analysis results for  $Ti_{50.0}Ni_{50.0}$  alloy after quenching (a) and cold rolling without current to  $\epsilon=0.7$  (b) with the overlay of tabular data corresponding to the  $C19'$  phase (green lines)

**B2** austenite becomes the main phase, although martensitic peaks are present in small amounts (Fig. 3, *b*). This reverse *MT* is typical for the alloy in the martensitic state after large strain [40], and it is associated with an increase in dislocation density, which stabilizes the austenite [41].

The reverse transformation from martensite to austenite induced by strain was first observed in [42] and later confirmed in [43]. This transformation is observed after large plastic deformations and precedes the onset of amorphization. The authors attribute the phenomenon to a change from sliding and twinning mechanisms to rotational deformation modes. According to [40], the **B2** phase is more resistant to large strain, while the **B19'** phase is susceptible to disordering with the accumulation of crystalline structure defects.

The reverse strain-induced *MT*, “martensite **B19'** → austenite **B2**” is also observed after pulsed current-assisted rolling to a small strain ( $\epsilon = 0.4$ ) in the  $Ti_{50.0}Ni_{50.0}$  alloy. The **B2** phase becomes the dominant phase (Fig. 4). In addition to the reasons mentioned above, it should be noted that short-term, localized electrical heating is possible in this study. This localized heating may be sufficient to induce the “martensite **B19'** → austenite **B2**” transformation, because the characteristic temperatures of *MTs* are sensitive to even small amounts of heat, and the  $A_f$  temperature after rolling does not exceed 58 °C (Fig. 2, *a*).

A further increase in strain up to  $\epsilon = 0.8$  in the  $Ti_{50.0}Ni_{50.0}$  alloy during pulsed current-assisted rolling leads to a stress increase in the newly formed austenitic phase. The accumulation of these stresses provides a mechanism for the direct *MT* (austenite **B2** → martensite **B19'**) to occur. Concurrently, there is a noticeable increase in the relative intensity of the martensitic diffraction pattern peaks, indicating an increasing proportion of the martensitic phase (Fig. 4). A subsequent increase in strain to  $\epsilon = 1.4$  again results in the main peak from the **B2** phase becoming the most pronounced. This indicates a reverse strain-induced *MT* from the previously formed martensite, the mechanisms of which are dominated by the thermal action of the current. Thus, a cyclical martensitic transformation is observed in the  $Ti_{50.0}Ni_{50.0}$  alloy during pulsed current-assisted rolling. The underlying reason is the alternating dominance of deformation mechanisms (stress increase in the austenitic phase due to strain) and heating from the pulsed current.

In the  $Ti_{50.0}Ni_{50.0}$  alloy, **B2** austenite remained the dominant phase during pulsed current-assisted rolling, as it was in the initial quenched state (Fig. 5). There was no evidence of strain-induced martensite, which is typically observed in *Ni*-rich alloys during deformation [37]. Such strain-induced martensite usually results from a shift in the reverse *MT* temperatures to higher values (the effect of martensite stabilization by preliminary deformation [44]). A possible reason for its absence during rolling with current may be short-term, localized heating. Apparently, in this case, the thermal effect of the current dominates the mechanisms of strain-induced martensite formation, leading to high-temperature **B2** austenite stabilization.

A notable feature of the diffraction patterns from samples after rolling with current is the broadening of the main **B2** (110) peak (Fig. 5, *b*, inset). This broadening is due to an increase in defects with increasing strain, as well as the presence of a pronounced peak corresponding to titanium oxides. In this case, the broadening of the main peak is logically associated with an increase in microstrains in the crystal lattice due to deformation. Oxide particles are frequently observed and studied by other authors in shape memory alloys [37, 45]. These particles enter the alloy during the smelting stage and are almost always present in

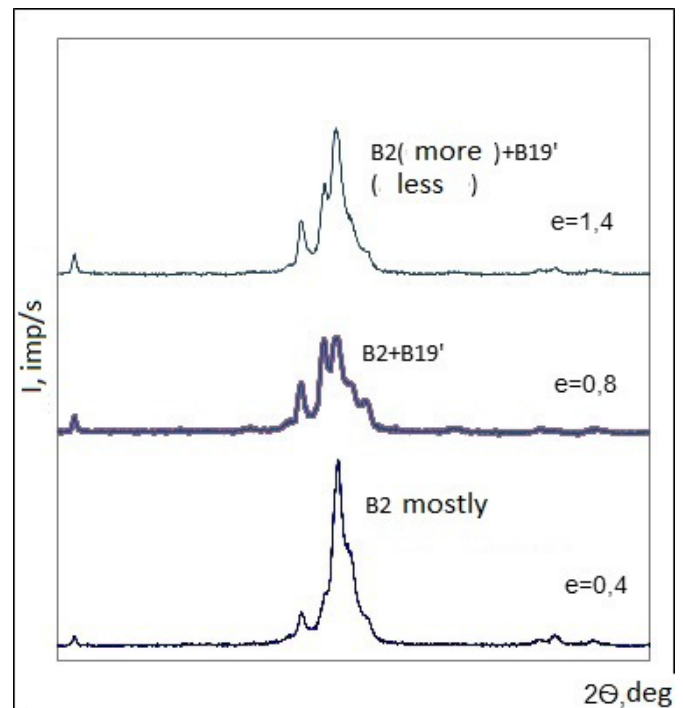


Fig. 4. X-ray diffraction analysis results for  $Ti_{50.0}Ni_{50.0}$  alloy after current-assisted rolling to various strain levels ( $\epsilon$ )



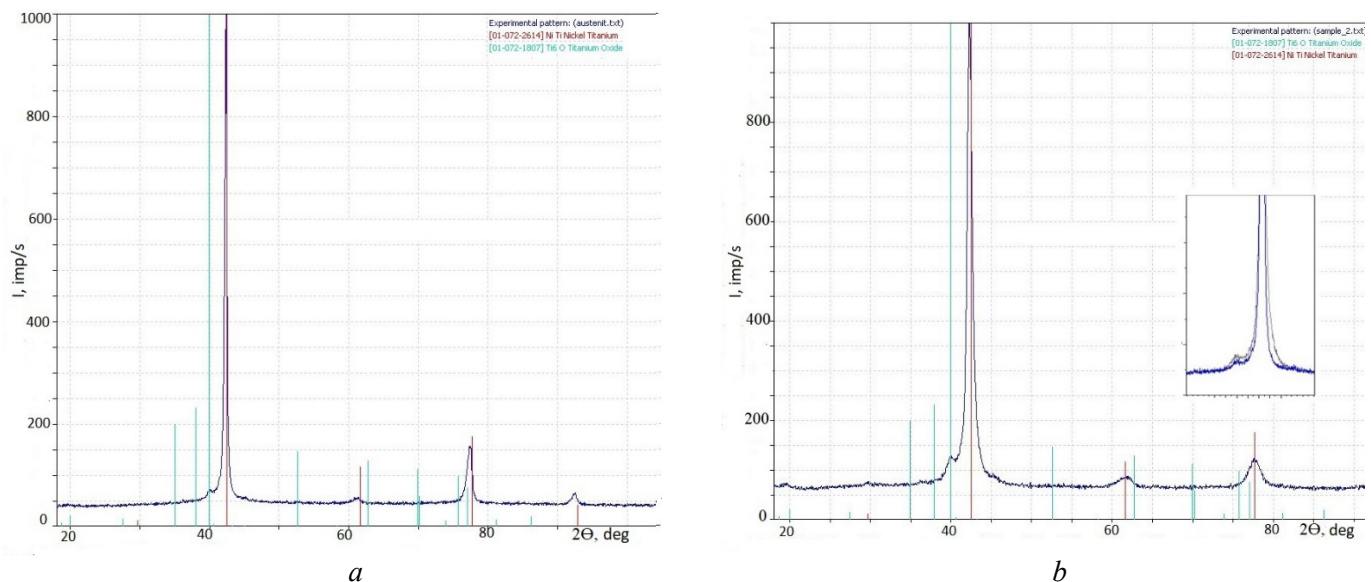


Fig. 5. X-ray diffraction analysis results for  $Ti_{49.2}Ni_{50.8}$  alloy after quenching from 800 °C in water (a) and current-assisted rolling to  $\varepsilon=0.4$  (b) with an overlay of tabular data corresponding to the B2 phase (red lines) and  $Ti_4Ni_2O$  particles (green lines); inset: comparison of the broadening of the main B2 (110) peak after quenching (blue) and current-assisted rolling,  $\varepsilon=0.4$  (grey)

its composition. The broadening of the corresponding X-ray peak may indicate their crushing by pulsed current-assisted rolling, but the thermal effect of the current is insufficient to dissolve them.

Microstructural studies using TEM reveal significant fragmentation of the initial grains after pulsed current-assisted rolling up to  $\varepsilon = 0.4$  in the  $Ti_{49.2}Ni_{50.8}$  alloy (Fig. 6, a). Deformation shear bands are observed within the structure, primarily oriented along the rolling direction. The thickness of these bands ranges from approximately 500 nm (most commonly observed) (Fig. 6, b) to 30 nm (Fig. 6, c). After straining to  $\varepsilon = 1.4$ , the microstructure exhibits a similar grain morphology but is more homogeneous. In this condition, thin shear bands (approximately 20-30 nm thick) are observed within wider (400-500 nm) deformation bands (Fig. 6, d).

Fig. 7 presents the TEM results for the  $Ti_{50.0}Ni_{50.0}$  alloy during pulsed current-assisted rolling up to  $\varepsilon = 0.8$  and 1.4. These results indicate that deformation in this alloy occurs through twinning of the initial martensitic plates. The bright-field structure image after straining to  $\varepsilon = 0.8$  is characterized by the presence of thin (20-30 nm) deformation bands. The electron diffraction pattern exhibits double reflections (Fig. 7, a). As strain increases to  $\varepsilon = 1.4$ , the deformation bands become even thinner, reaching thicknesses of less than 10 nm. The electron diffraction pattern corresponding to this state is characterized by reflections that are elongated along a circle, indicating strong lattice distortions after pulsed current-assisted rolling. The arrangement of the rings is typical for the B2 austenite phase; however, some areas exhibit martensitic reflections (reflections with similar interplanar distances near (110)) (Fig. 7, b). A comparison of the deformation process during pulsed current-assisted rolling for the TiNi-based alloys, considering their initial austenitic and martensitic structures, reveals that the  $Ti_{50.0}Ni_{50.0}$  alloy undergoes more intense deformation. This observation is supported by the results of X-ray diffraction analysis.

Thus, a characteristic feature of structure formation in the  $Ti_{50.0}Ni_{50.0}$  alloy is the cyclical nature of the direct and reverse “martensite  $\rightarrow$  austenite  $\rightarrow$  martensite” transformations during pulsed current-assisted rolling. A possible explanation for this phenomenon is the alternating dominance of strain-induced martensitic transformation mechanisms and the localized influence of the thermal action of the current on the characteristic martensitic transformation temperatures. In contrast, a special characteristic of the effect of pulsed current during rolling on martensitic transformations in the  $Ti_{49.2}Ni_{50.8}$  alloy is the absence of strain-induced martensite B19' and the stabilization of the high-temperature austenitic B2 phase. These distinct features of MT manifestation can be utilized to control the structural and phase state of shape memory alloys in order to maximize functional properties such as reversible strain, recovery stress, and superelasticity.

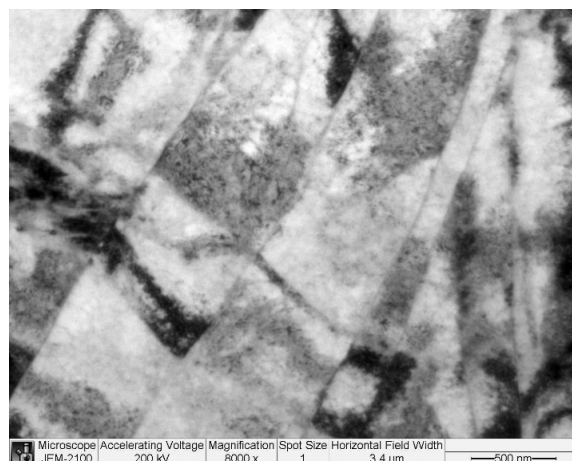
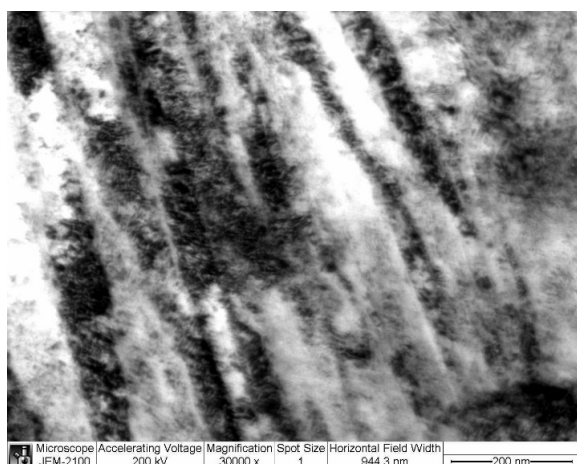
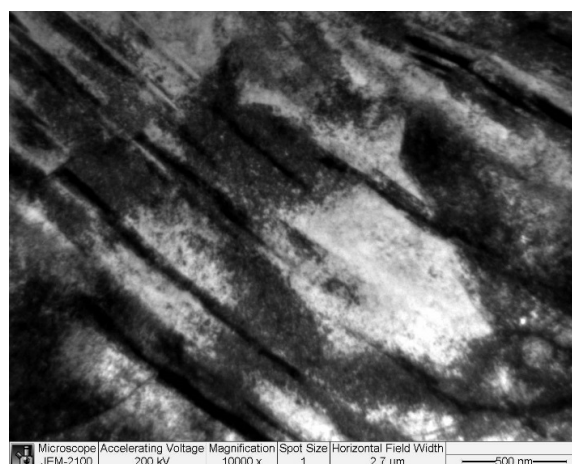
*a**b**c**d*

Fig. 6. Transmission electron microscopy images of  $Ti_{49.2}Ni_{50.8}$  alloy after current-assisted rolling to  $\epsilon=0.4$  at various magnifications:  $\times 6000$  (a),  $\times 8000$  (b),  $\times 30000$  (c); and to  $\epsilon=1.4$  (d)

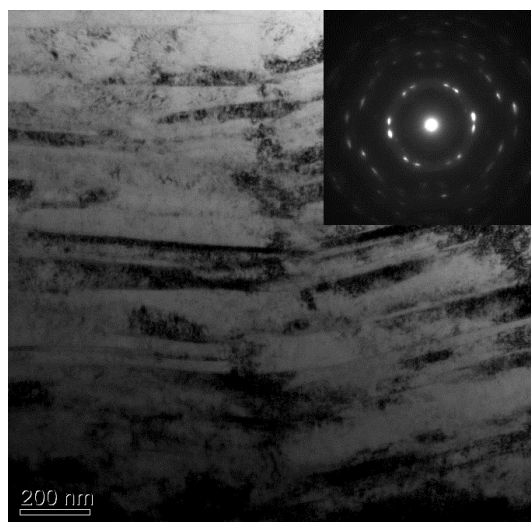
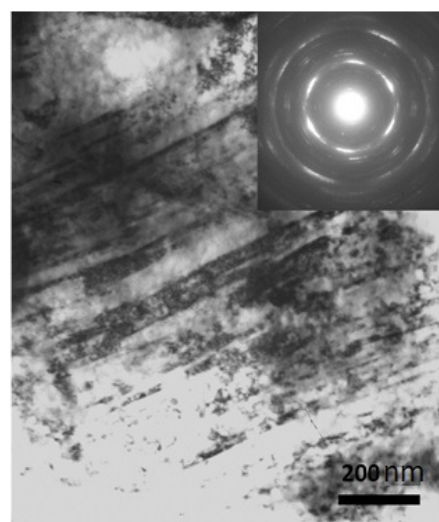
*a**b*

Fig. 7. Transmission electron microscopy images of  $Ti_{50.0}Ni_{50.0}$  alloy during current-assisted rolling: to  $\epsilon=0.8$  (a); to  $\epsilon=1.4$  (b)

## Conclusion

– Pulsed current-assisted rolling and post-deformation annealing at 450 °C alters the direct thermal martensitic transformation pathway upon cooling, from  $B2 \rightarrow B19'$  to  $B2 \rightarrow R \rightarrow B19'$ , in both the initially single-phase martensitic ( $Ti_{50.0}Ni_{50.0}$ ) and austenitic ( $Ti_{49.2}Ni_{50.8}$ ) alloys in the quenched state. Increasing the strain during pulsed current-assisted rolling expands the temperature range over which the  $R$ -phase exists.

– A cyclic strain-induced “martensite  $\rightarrow$  austenite  $\rightarrow$  martensite” transformation was detected in the  $Ti_{50.0}Ni_{50.0}$  alloy during pulsed current-assisted rolling. This behavior is attributed to the alternating dominance of deformation mechanisms and the localized thermal influence of the current on the characteristic martensitic transformation temperatures.

– The effect of pulsed current-assisted rolling on martensitic transformations in the  $Ti_{49.2}Ni_{50.8}$  alloy is characterized by the absence of strain-induced  $B19'$  martensite and the stabilization of the high-temperature austenitic  $B2$  phase.

## References

1. Brailovski V., Prokoshkin S., Terriault P., Trochu F. *Shape memory alloys: fundamentals, modelling and applications*. Montreal, University of Quebec, 2003. 844 p.
2. Tsuchiya K., Ahadi A. Anomalous properties of TiNi processed by severe plastic deformation. Sun Q., Matsui R., Takeda K., Pieczyska E. (eds.). *Advances in Shape Memory Materials. Advanced Structured Materials*, vol. 73. Cham, Springer, 2017, pp. 191–201. DOI: 10.1007/978-3-319-53306-3\_14.
3. Andreev V.A., Karelin R.D., Komarov V.S., Cherkasov V.V., Dormidontov N.A., Laisheva N.V., Yusupov V.S. Influence of rotary forging and post-deformation annealing on mechanical and functional properties of titanium nickelide. *Metallurgist*, 2024, vol. 67, pp. 1912–1919. DOI: 10.1007/s11015-024-01688-4.
4. Shuitcev A.V., Ren Y., Gunderov D.V., Vasin R.N., Li L., Valiev R.Z., Zheng Y.F., Tong Y.X. Grain growth in  $Ni_{50}Ti_{30}Hf_{20}$  high-temperature shape memory alloy processed by high-pressure torsion. *Materials Science and Engineering: A*, 2024, vol. 918, p. 147478. DOI: 10.1016/j.msea.2024.147478.
5. Andreev V.A., Yusupov V.S., Perkas M.M., Yakushevich N.V. Goryachaya rotatsionnaya kovka prutkov diametrom 2–20 mm iz splavov s pamyat'yu formy na osnove nikelida titana [Hot rotary forging of bars with a diameter of 2–20 mm from shape memory alloys based on titanium nickelide]. *Perspektivnye materialy i tekhnologii*. V 2 t. T. 1 [Promising materials and technologies. In 2 vol. Vol. 1]. Vitebsk, Vitebsk State Technological University Publ., 2017, pp. 61–69.
6. Andreev V.A., Karelin R.D., Komarov V.S., Cherkasov V.V., Dormidontov N.A., Laisheva N.V., Yusupov V.S. Vliyanie rezhimov rotatsionnoi kovki i posledeformatsionnoi termicheskoi obrabotki na mekhanicheskie i funktsional'nye svoistva nikelida titana [Influence of rotary forging and post-deformation heat treatment on mechanical and functional properties of titanium nickelide]. *Metallurg = Metallurgist*, 2023, no. 12, pp. 87–92. DOI: 10.52351/00260827\_2023\_12\_87. (In Russian).
7. Lotkov A.I., Grishkov V.N., Baturin A.A., Dudarev E.F., Zhapova D.Yu., Timkin V.N. Vliyanie teploi deformatsii metodom abc-pessovaniya na mekhanicheskie svoistva nikelida titana [The effect of warm deformation by abc-pressing method on mechanical properties of titanium nickelide]. *Pis'ma o materialakh = Letters on Materials*, 2015, vol. 5 (2), pp. 170–174. DOI: 10.22226/2410-3535-2015-2-170-174. (In Russian).
8. Fedotkin A.A., Stolyarov V.V. Osobennosti deformatsionnogo povedeniya nanostrukturnykh titanovykh splavov pri rastyazhenii pod deistviem impul'snogo toka [Features of the deformation behavior of nanostructured titanium alloys under tension under the action of pulsed current]. *Mashinostroyeniye i inzhenernoye obrazovaniye = Mechanical Engineering and Engineering Education*, 2012, no. 1 (30), pp. 28–35.
9. Misochenko A.A., Fedotkin A.A., Stolyarov V.V. Influence of grain size and electric current regimes on deformation behavior under tension of shape memory alloy  $Ti_{49.3}Ni_{50.7}$ . *Materials Today: Proceedings*, 2017, vol. 4 (3), pp. 4753–4757. DOI: 10.1016/j.matpr.2017.04.065.
10. Stolyarov V.V. Elektroplasticheskiy effekt v krupnozernistom i ul'tramelkozernistom titane [The electroplastic effect in coarse-grained and ultrafine-grained titanium]. *Zavodskaya laboratoriya. Diagnostika materialov = Industrial laboratory. Diagnostics of materials*, 2023, vol. 89 (8), pp. 62–66. DOI: 10.26896/1028-6861-2023-89-8-62-66. (In Russian).





11. Khalik M.A., Zahiri S.H., Masood S.H., Palanisamy S., Guliz S. In situ electro-plastic treatment for thermomechanical processing of CP titanium. *The International Journal of Advanced Manufacturing Technology*, 2021, vol. 115, pp. 2639–2657. DOI: 10.1007/s00170-021-07342-6.
12. Baranov Yu.V., Troitskii O.A., Avraamov Yu.S., Shlyapin A.D. *Fizicheskie osnovy elektroimpul'snoi i elektroplasticheskoi obrabotki i novye materialy* [Physical foundations of electric pulse and electroplastic treatments and new materials]. Moscow, MSIU Publ., 2001. 844 p.
13. Jiang B., Yang W., Zhang Z., Li X., Ren X., Wang Y. Numerical simulation and experiment of electrically-assisted incremental forming of thin TC4 titanium alloy sheet. *Materials*, 2020, vol. 13 (6), p. 1335. DOI: 10.3390/ma13061335.
14. Xu Z., Jiang T., Huang J., Peng L., Lai X., Fu M.W. Electroplasticity in electrically-assisted forming: process phenomena, performances and modelling. *International Journal of Machine Tools and Manufacture*, 2022, vol. 175, p. 103871. DOI: 10.1016/j.ijmachtools.2022.103871.
15. Dobras D., Zimniak Z., Zwierzchowski M. Electrically-assisted deep drawing of 5754 aluminum alloy sheet. *Materials Research Proceedings*, 2023, vol. 28, pp. 987–1006. DOI: 10.21741/9781644902479-109.
16. Herbst S., Karsten E., Gerstein G., Reschka S., Nürnberger F., Zaefferer S., Maier H.J. Electroplasticity mechanisms in hcp materials. *Advanced Engineering Materials*, 2023, vol. 25, p. 2201912. DOI: 10.1002/adem.202201912.
17. Rudolf C., Goswami R., Kang W., Thomas J. Effects of electric current on the plastic deformation behavior of pure copper, iron, and titanium. *Acta Materialia*, 2021, vol. 209, p. 116776. DOI: 10.1016/j.actamat.2021.116776.
18. Stolyarov V., Calliari I., Gennari C. Features of the interaction of plastic deformation and pulse current in various materials. *Materials Letters*, 2021, vol. 299, p. 130049. DOI: 10.1016/j.matlet.2021.130049.
19. Potapova A.A., Stolyarov V.V. Deformability and structural features of shape memory TiNi alloys processed by rolling with current. *Materials Science and Engineering: A*, 2013, vol. 579, pp. 114–117. DOI: 10.1016/j.msea.2013.05.003.
20. Stolyarov V.V., Andreev V.A., Karelin R.D., Ugurchiev U.Kh., Cherkasov V.V., Komarov V.S., Yusupov V.S. Deformability of TiNiHf shape memory alloy under rolling with pulsed current. *Obrabotka metallov (tekhnologiya, oborudovanie, instrumenty) = Metal Working and Material Science*, 2022, vol. 24 (3), pp. 66–75. DOI: 10.17212/1994-6309-2022-24.3-66-75.
21. Zhu R., Tang G. The improved plasticity of NiTi alloy via electropulsing in rolling. *Materials Science and Technology*, 2016, vol. 33 (5), pp. 1743–2847. DOI: 10.1080/02670836.2016.1231745.
22. Potapova A.A., Resnina N.N., Stolyarov V.V. Shape memory effects in TiNi-based alloys subjected to electroplastic rolling. *Journal of Materials Engineering and Performance*, 2014, vol. 23 (7), pp. 2391–2395. DOI: 10.1007/s11665-014-1046-0.
23. Zhu R.F., Jiang Y.B., Guan L., Li H.L., Tang G.Y. Difference in recrystallization between electropulsing-treated and furnace-treated NiTi alloy. *Journal of Alloys and Compounds*, 2016, vol. 658, pp. 548–554. DOI: 10.1016/j.jallcom.2015.10.239.
24. Stolyarov V., Misochenko A. A pulsed current application to the deformation processing of materials. *Materials*, 2023, vol. 16 (18), p. 6270. DOI: 10.3390/ma16186270.
25. Sheng Y., Hua Y., Wang X., Zhao X., Chen L., Zhou H., Wang J., Berndt C.C., Li W. Application of high-density electropulsing to improve the performance of metallic materials: mechanisms, microstructure and properties. *Materials*, 2018, vol. 11 (2), p. 185. DOI: 10.3390/ma11020185.
26. Ghiotti A., Bruschi S., Simonetto E., Gennari C., Calliari I., Bariani P. Electroplastic effect on AA1050 aluminium alloy formability. *CIRP Annals*, 2018, vol. 67 (1), pp. 289–292. DOI: 10.1016/j.cirp.2018.04.054.
27. Li X., Tang G., Kuang J., Li X., Zhu J. Effect of current frequency on the mechanical properties, microstructure and texture evolution in AZ31 magnesium alloy strips during electroplastic rolling. *Materials Science and Engineering: A*, 2014, vol. 612, pp. 404–413. DOI: 10.1016/j.msea.2014.06.075.
28. Zhan L., Li R., Wang J., Xue X., Wang Y., Lv Z. Thermoelectric coupling deep drawing process of ZK60 magnesium alloys. *International Journal of Advanced Manufacturing Technology*, 2023, vol. 126, pp. 3005–3014. DOI: 10.21203/rs.3.rs-1791252/v1.
29. Liu Y., Fan J., Zhang H., Jin W., Dong H., Xu B. Recrystallization and microstructure evolution of the rolled Mg-3Al-1Zn alloy strips under electropulsing treatment. *Journal of Alloys and Compounds*, 2015, vol. 622, pp. 229–235. DOI: 10.1016/j.jallcom.2014.10.062.
30. Zhang W., Wang S., Pan J., Yang J. Extraordinary Bending Formability of Mg-2.5Nd-0.5Zn-0.5Zr alloy sheet through pulsed current. *Metals and Materials International*, 2023, vol. 29, pp. 3371–3384. DOI: 10.1007/s12540-023-01450-6.



31. Zhang R.K., Li X.H., Kuang J., Li X.P., Tang G.Y. Texture modification of magnesium alloys during electro-pulse treatment. *Materials Science and Technology*, 2017, vol. 33, pp. 1421–1427. DOI: 10.1080/02670836.2017.1291164.
32. Kuang J., Low T.S.E., Niezgoda S.R., Li X., Geng Y., Luo A.A., Tang G. Abnormal texture development in magnesium alloy Mg-3Al-1Zn during large strain electroplastic rolling: effect of pulsed electric current. *International Journal of Plasticity*, 2016, vol. 87, pp. 86–99. DOI: 10.1016/j.ijplas.2016.09.004.
33. Dobras D., Zimniak Z., Zwierzchowski M. The effect of pulsed electric current on the structural and mechanical behavior of 6016 aluminium alloy in different states of hardening. *Archives of Civil and Mechanical Engineering*, 2023, vol. 23, art. 166. DOI: 10.1007/s43452-023-00700-z.
34. Potapova A.A., Stolyarov V.V. Relaxation effect of pulse current on  $\text{Ti}_{50.0}\text{Ni}_{50.0}$  structure during rolling. *Materials Science and Technology*, 2015, vol. 31 (13), pp. 1541–1544. DOI: 10.1179/1743284715Y.0000000021.
35. Misochenko A.A., Stolyarov V.V. Teplovoe deistvie impul'snogo toka v splavakh s razlichnymi teplofizicheskimi svoistvami [Heat effect in the metals during electropulse treatment]. *Stankoinstrument*, 2023, no. 4 (33), pp. 34–41. DOI: 10.22184/2499-9407.2023.33.4.34.41. (In Russian).
36. Database of the International Diffraction Data Center (ICDD) PDF-2 (2024). Available at: <https://www.icdd.com/pdf-2/> (accessed 07.12.2024).
37. Pushin V.G., Kondrat'ev V.V., Khachin V.N. *Predperekhodnye yavleniya i martensitnye prevrashcheniya* [Pre-transition phenomena and martensitic transformations]. Yekaterinburg, Ural Branch of the Russian Academy of Sciences Publ., 1998. 368 p.
38. Pelton A.R., Huang G.H., Moinec P., Sinclair R. Effects of thermal cycling on microstructure and properties in Nitinol. *Materials Science and Engineering: A*, 2012, vol. 532, pp. 130–138.
39. Komarov V., Khmelevskaya I., Karelin R., Kawalla R., Korpala G., Prah U., Yusupov V., Prokoshkin S. Deformation behavior, structure and properties of an equiatomic Ti–Ni shape memory alloy compressed in a wide temperature range. *Transactions of the Indian Institute of Metals*, 2021, vol. 74, pp. 2419–2426. DOI: 10.1007/s12666-021-02355-x.
40. Surikova N.S., Litovchenko I.Yu., Korznikova E.A. Strukturnye prevrashcheniya v monokristallakh nikelida titana pri intensivnoi plasticheskoi deformatsii [Structure transformations in titanium nickelide single crystals under severe plastic deformation]. *Vestnik Tambovskogo universiteta. Seriya: Estestvennye i tekhnicheskie nauki = Tambov University Reports. Series: Natural and Technical Sciences*, 2013, vol. 18 (4-2), pp. 1966–1967.
41. Karelin R.D., Komarov V.S., Khmelevskaya I.Yu., Andreev V.A., Yusupov V.S., Prokoshkin S.D. [Formation of the structure and properties of Ti–Ni SPF after IPD by the RCUP method in a shell]. *Prochnost' neodnorodnykh struktur – PROST 2023* [Strength of heterogeneous structures – PROST 2023]. Proceedings of the XI Eurasian Scientific and Practical Conference. Moscow, 2023, p. 78. (In Russian).
42. Zel'dovich V.I., Frolova N.Yu., Pilyugin V.P., Gundyrev V.M., Patselov A.M. Formirovanie amorfnoi struktury v nikelide titana pri plasticheskoi deformatsii [Formation of amorphous structure in titanium nickelide under plastic deformation]. *Fizika metallov i metallovedenie = Physics of Metals and Metallography*, 2005, vol. 99 (4), pp. 90–100. (In Russian).
43. Frolova N., Zeldovich V., Pilyugin V., Gundyrev V., Patselov A. Amorphization of titanium nickelide by means of shear under pressure and crystallization at the subsequent heating. *Materials Science Forum*, 2013, vol. 738–739, pp. 525–529. DOI: 10.4028/www.scientific.net/MSF.738-739.525.
44. Belyaev S., Resnina N., Rakhimov T., Andreev V. Martensite stabilisation effect in Ni-rich NiTi shape memory alloy with different structure and martensitic transformations. *Sensors and Actuators A: Physical*, 2020, vol. 305, p. 111911. DOI: 10.1016/j.sna.2020.111911.
45. Frenzel J., George E.P., Dlouhy A., Somsen C., Wagner M.F.-X., Eggeler G. Influence of Ni on martensitic phase transformations in NiTi shape memory alloys. *Acta Materialia*, 2010, vol. 58 (9), pp. 3444–3458. DOI: 10.1016/j.actamat.2010.02.019.

## Conflicts of Interest

The author declare no conflict of interest.